Int. J. Electrochem. Sci., 11 **(2016)** 277 - 290

International Journal of
ELECTROCHEMICAL
SCIENCE
www.electrochemsci.org

Effect of the Microstructures Formed in Cements Modified by Limestone Agave Bagasse Ash, Fly Ash, Geothermal Nano-SiO_2 Waste and Silica Fume on Chloride Ion Penetration Resistance

R. Puente-Ornelas[1,], L. Chávez Guerrero[1], G. Fajardo-San Miguel[2], E. A. Rodríguez[1], A. Trujillo-Álvarez[1], H. E. Rivas-Lozano[1], H. M. Delgadillo-Guerra[1].*

[1] Universidad Autónoma de Nuevo León, Facultad de Ingeniería Mecánica y Eléctrica, Centro de Investigación y Desarrollo Tecnológico, Av. Universidad S/N. Ciudad Universitaria. San Nicolás de los Garza, Nuevo León, México. C.P. 66455.
[2] Universidad Autónoma de Nuevo León, Facultad de Ingeniería Civil, Av. Universidad S/N. Ciudad Universitaria. San Nicolás de los Garza, Nuevo León, México. C.P. 66455.
[*]E-mail: ropuor@gmail.com

Received: 30 September 2015 / *Accepted:* 28 October 2015 / *Published:* 1 December 2015

In the present work, pastes were fabricated replacing the ordinary portland cement (OPC) by 0, 1.67, 2.5 and 5 wt% of limestone from agave bagasse ash (ABA), fly ash (FA), geothermal nano-SiO_2 waste (GNW) and silica fume (SF), using 1.5 wt% of superplasticizer based in carboxylate and a water/binder ratio of 0.45. After fabrication, the pastes were cured at 20ºC and a humidity content of 100% for up to 28 days. The compressive strength, chloride penetration, porosity and microstructural evolution properties were evaluated. The results obtained from the test suggests that the mechanical, electrochemical, physical and microstructural properties resulting from the cured specimens were enhanced, when compared to the cements obtained with pastes composed by 100% of OPC. It was found that the ABA pastes improved by ~15% to ~25% their mechanical resistance, compared with the values obtained for 100% OPC and 5% FA respectively. Additionally, the pastes containing 2.5% of ABA and 2.5% of GNW, showed an increase of 35% in the values of mechanical resistance in comparison to the 100% OPC. It is also worth mentioning that a the pastes experienced a higher densification value, mainly due to the addition of GNW, which promotes the development of a matrix with reduced porosity when compared with values measured at 100% OPC. The chlorine ion penetration ratio had also low values giving an ion penetration resistance around 57 % less. These results revealed that geothermal nano-SiO_2 waste (GNW) and limestone of agave bagasse ash (ABA) could be considered as a potentially suitable material for making pastes, mortars and concrete for industrial applications, which will contribute positively to the reduction of the CO_2 emissions into the atmosphere, as well as decrease the environmental impact generated at the disposal zones.

Keywords: Chloride ion, cement, limestone, nano-SiO_2, microstructure.

1. INTRODUCTION

Current problems caused by the high emissions of CO_2, such as global warming and the increase in the generation of industrial wastes have created conscience in society about the environment preservation. Moreover, cement sustainability has been threatened by the increase in the price of fossil fuels and eco-taxes for the release of CO_2. Following from the above mentioned, the mitigation of CO_2 emissions through the use of mineral admixtures as cement replacement is nowadays a common practice [1-2], not only to preserve the environment, energy and natural resources, but also to improve the quality, properties (physical, chemical, mechanical), durability and price of concrete [4-5].

There are many research in which mineral admixtures have been used such as natural puzzolans, limestone filler, industrial wastes (granulated blast furnace slag, fly ash, silica fume and rice hush ash), coarse recycled concrete aggregates to name a few [6-10]. In several cases, these replacements increase the mechanical strength and enhance the microstructural uniformity with a reduction in permeability and porosity.

In spite of many reports related to the use of mineral admixtures in the last five decades, those can replace a definite percentage of cement without impairing the properties of concrete, but there is a little information about the use of industrial wastes generated by geothermal plants and mezcal or tequila industry. In the case of the wastes generated by geothermal power plants, these cause important problems due to their generation and accumulation. Several estimations indicated that over 80% of the existing plants have these difficulties [11]. Nevertheless, currently the production of electricity through geothermal resources is growing by the economic and ecological advantages provided in comparison with other sources of electricity generation [12].

One of these plants is located in Baja California, Mexico, producing up to 70,000 tons per year [12] of the wastes (called geothermal nanosilica waste, GNW) above mentioned, so it is important to find an application for this "waste". The GNW is a material composed by amorphous silica nanoparticles (~20nm) in more than 90 wt.% and considerable amounts of sodium and potassium chlorides [14]. This material has been studied as secondary material in the production of glass, ceramics and refractory [14] as well as in the preparation of pastes, mortars and concretes [16-18].

In the other hand, the mezcal and tequila industry, which is an alcoholic beverage produced in Mexico, requires agave plants as raw materials for manufacturing, whose consumption has increased over 1,000,000 tons per year [19]. According to Ibarra-Hernandez et al [20], the overall composition of the agave plant is: (water) humidity 60%, 25% carbohydrates, fiber 10%, minerals 2.5% and 2.5% of other components such as proteins and inulins, so therefore, during the manufacturing process for producing mezcal or tequila they are producing thousands of tons of waste which is commonly called bagasse, which is only in the production of industry mezcal generates of 15-20 kg per liter [21]. If this waste is not recycled or appropriately processed, pollution is generated. Waste is usually burned or dumped in landfills.

According to various studies, the bagasse is a candidate for use in health remedies, construction, fertilizer, fuel and as substrates for enzymes inulinases for microorganisms as Aspergillus niger CH-A-2010 and CH-A-2016 [22-27]. However, there are few studies on the

feasibility of use in the construction industry [28-29]. For this reason, in the present research were studied the effects of replacement of ordinary portland cement by limestone of agave bagasse ash, fly ash, geothermal nano-SiO_2 waste and silica fume in the porosity, mechanical strength, microstructure and resistance to chloride ion penetration of pastes elaborated with these materials. The above, venture into new trends in the development and improvement of materials alternative to cement, thus seeks preservation environment.

2. EXPERIMENTAL PROCEDURE

2.1. Raw materials

The agave bagasse used in this research was collected direct from the mezcal factory IPIÑA S.A de C.V. in San Luis Potosí, México. A Thermolyne 48000 furnace was used to heat the bagasse at 450°C to obtain limestone of agave bagasse ash (ABA). The ash was sieved to obtain a powder less than 75 μm and finally homogenized. The fly ash (FA) provided by the Thermoelectric José López Portillo plant (located in Nava , Coahuila, Mexico) which it is class F, due to their low content of CaO, according to what is described by ASTM C618-08a [30], was sieved to obtain particles below 75 μm and finally homogenized.

Table 1. Chemical composition of the cementitious materials (wt%).

	OPC	GNW	FA	ABA	SF
Na_2O	0.36	0.32	0.273	-	0.17
MgO	1.27	-	0.845	15.79	0.42
Al_2O_3	4.46	0.09	25.144	-	0.42
SiO_2	18.51	98.36	61.165	1.40	95.89
P_2O_5	0.08	-		3.53	0.06
SO_3	3.26	0.03	0.184	0.82	0.45
Cl^-	-	0.06		-	-
K_2O	0.87	0.23	1.405	12.75	0.41
CaO	67.45	0.45	2.420	65.31	0.61
TiO_2	0.21	-	0.988	-	-
Mn_2O_3	0.13	0.05	0.014	-	0.03
Fe_2O_3	2.61	0.04	4.556	0.189	1.22
Loss of ignition	0.79	0.31	3.016	0.21	0.29
Insoluble residues	-	0.05	-	-	0.03
Total	**100.00**	**100.00**	**100.00**	**100.00**	**100.00**

The geothermal nano-SiO_2 waste (GNW) provided by the geothermal plant of Cerro Prieto (located in Baja California, North of Mexico) was washed in water at 100°C because it contained high concentrations of sodium and potassium chlorides (~32.2%). This washing was done in order to obtain the desired concentrations of total chloride of 0 wt%. The % of total chlorides (Cl^-) with respect to the cement weight, were determined via volumetric titration using the Mohr method [31]. After washing,

the GNW was filtered and then dried for 24 h at 120°C in an electrical oven. Subsequently the GNW was sieved to obtain particles below 75 μm and finally homogenized.

The cement used in this study was provided by CEMEX Mexico and corresponds to the classification of OPC type I (Ordinary Portland Cement the current standard Mexican cement in Mexico, NMX-C-414-ONNCCE [32]). All raw materials used in this study were characterized by X-ray fluorescence and the chemical compositions are shown in Table 1.

2.2. Mix design and production of pastes

Cylindrical pastes were prepared under different mixtures design using ordinary portland cement type I, limestone of agave bagasse ash (ABA), fly ash (FA), geothermal nano-SiO_2 waste (GNW), silica fume, distilled water and a commercial superplasticizers (glenium 3150, based polycarboxylate) in a ratio of 1.5 wt% of cementitious materials. The dimensions of the cylindrical pastes were 25.4x50.5mm and were prepared using a ratio water/cementitious materials (w/cm) of 0.45, as well as the replacement of OPC by 1.67, 2.5 and 5 wt% of cementitious materials (ABA, FA, GNW and SF). Dosage of raw materials used is shown in Table 2. The pastes were set at 20ºC. After 24 hours the pastes were placed in plastic containers with calcium hydroxide saturated water and cured up to 28 days using a temperature of 20°C. In order to obtain the best reproducibility, four pastes were used for every type of mixtures and each hydration period.

Table 2. Mix proportions of pastes fabricated (wt%).

		Supplementary Cementing Material (Replacement level of OPC %)						
	OPC	**ABA**	**FA**	**GNW**	**SF**	**Water**	**SP**	**Total**
R	68.26 (100%)	-	-	-	-	30.72	1.02	**100**
M1	64.85 (95%)	3.41 (5%)	-	-	-	30.72	1.02	**100**
M2	64.85 (95%)	-	3.41 (5%)	-	-	30.72	1.02	**100**
M3	64.85 (95%)	-	-	3.41 (5%)	-	30.72	1.02	**100**
M4	64.85 (95%)	-	-	-	3.41 (5%)	30.72	1.02	**100**
M5	64.85 (95%)	1.71 (2.5%)	1.71 (2.5%)	-	-	30.72	1.02	**100**
M6	64.85 (95%)	1.14 (1.67%)	1.14 (1.67%)	1.14 (1.67%)	-	30.72	1.02	**100**

2.3. Measurement methods

The compressive strength was evaluated up 28 days in a compression machine of 200Tons for each one of cured ages. After the compressive strength tests, the center of the pastes was extracted and crushed to particles of approximately 5 mm diameter and placed in vacuum dried at 50°C for 24 h using acetone to stop reactions. For the analysis of pastes by Scanning Electron Microscopy (SEM), the representative samples were vacuum impregnated with epoxy resin, ground and polished down to ¼ μm using diamond pastes, and finally coated with carbon. The images in SEM were obtained in

backscattered electrons mode (BSE) at an accelerating voltage of 20 kV, the most relevant observations are presented in this paper. In addition, some sections of the pastes were taken to undergo there the test of the porosity following the procedure reported in the ASTM C-642-97 [33].

The resistance chloride ion penetration was evaluated in cylindrical pastes cured at 28 days according to the use of rapid chloride penetration test (RCPT) in agreement with ASTM C 1202. For that, the pastes of the dimensions 25.4x50.5mm were covered with epoxy paint in the periphery surface and after drying 24 hours, were introduced in a dryer chamber to a vacuum pressure of 1mm Hg for three hours; then, the chamber was filled with distilled water maintaining the vacuum pressure for 1 hour; then, the pastes were maintained in the immersion for 24 hours without chamber pressure. After a period of immersion, the pastes were placed between two cells connected to a potentiostat. After that, one of the cells was filled with aqueous solution prepared at 0.3 N of NaOH and the other cell with aqueous solution prepared at 3% of NaCl. Finally, the cells were connected to the voltage supply source, where the cell electrode with NaCl functioned as cathode and the NaOH electrode functioned like anode. The test of RCPT was carried out on 3 specimens per mix design, in order to obtain reproducible results, using a constant voltage of 60.0 ± 0.1 V for six hours obtaining as a result from the test a total passed charge (Q in coulombs). The results shown in the Q values (see figure 2) represent the average of three specimens of each mix design tested and are plotted according to the criteria suggested by the ASTM C1202 standard [34] (see table 3).

Table 3. Chloride ion penetrability based on charge passed.

Charge passed (coulombs)	Chloride Ion Penetrability
›4,000	High
2,000-4000	Moderate
1,000-2,000	Low
100-1,000	Very Low
‹100	Negligible

After the rapid chloride penetration test (RCPT), the pastes were broken in half to expose an internal cross section with aqueous solution prepared at 0.1 M of silver nitrate ($AgNO_3$) as indicator. After that, white silver chloride precipitation (AgCl) on the split surface appeared clearly after 5 min, thus revealing the presence of chloride ions within the paste. Subsequently, the depth of penetration of chloride ions was measured.

3. RESULTS AND DISCUSSION

The figure 1 show the obtained results in the compression resistance testing made in the pastes. In general, we can see an increase in the mechanical resistance with the different kinds of mixtures according with the curing age, due to of water reaction with the different stages of anhydrous cement to produce calcium hydroxide and CSH gel, being the last one the main promoter of mechanical strength. Also, the materials as FA, SF and GNW also fomenting an increase in the mechanical

properties of the pastes that was adding with these materials, since they reacted with calcium hydroxide to produce more CSH gel, so that after 28 days the vales of compressive strength of added pastes with 100% of OPC.

At 28 days, the pastes with GNW outnumbered pastes with 100% of OPC (mixture R) in 21.27%, 35.08% and 43.07% more in compressive strength to replace the OPC for GNW in 1.67% (mixture M6), 2.5 (mixture M5) and 5% (mixture M3) respectively. These results are attributed to the effectiveness of the pozzolanic reaction from GNW, so that more GNW in the cementitious matrix, it gives more likelihood to produce more CSH gel, and then, constantly the matrix will be compacted, enhancement the compressive strength values. A high pozzolanic activity has been observed in others investigations in which geothermal nanosilica were used as replacement material in cement [35,36]. In addition, it is important to note that according to studies by Quercia [37], which in turn refers to Qing [38] and Lin [39], the particles of nanosilica used in the production of mortars and concretes act as nucleation sites for gel CSH precipitation, achieving with it an improvement in the results of compressive strength, effect also observed with the use of GNW.

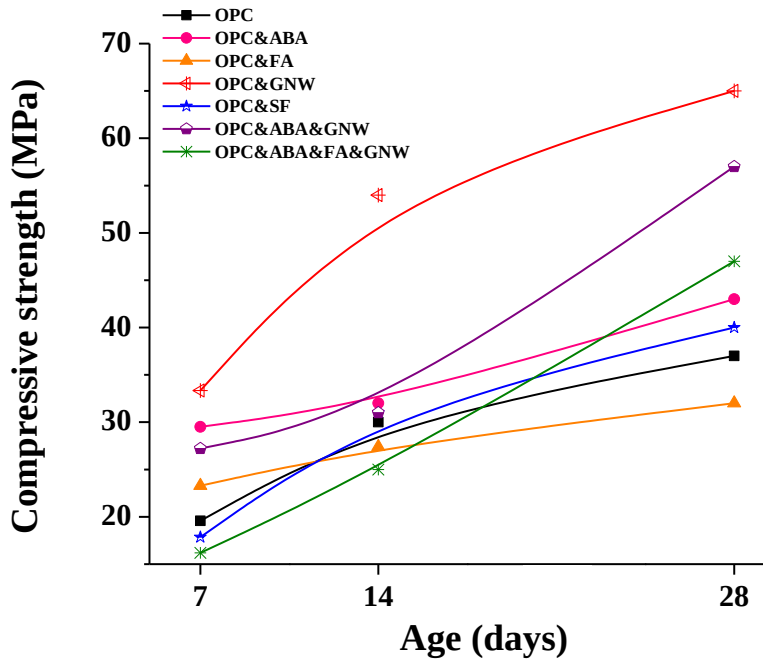

Figure 1. Results of compressive strength of pastes at 7, 14 and 28 days of curing.

Furthermore, it can be seen that the compressive strength of the produced pastes with 5% FA (mixture M2) is gradually increasing with time; however the resistance to 28 days is 13.52% lower than that exhibited by the R pastes. This phenomenon has been observed in pastes elaborated with OPC, which were added with fine spherical FA particles showing an increase in their mechanics resistance in later stages, this effect is attributed to packaging promoted by small and spherical fine fly ash particle so that their reaction is delayed at an early age [40-43].

Also, other authors who report that the size and spherical morphology, chemical composition and the amorphous fraction of the fly ash, modify the development of mechanical, chemical and microstructural properties of pastes, mortars and concretes [44]. Under this scheme, considering the observed in the investigation, would expected to at later ages, the M2 pastes will have greater compressive strength with respect to the R pastes.

Also in the figure 1 shows the pastes elaborated with 5% of SF (mixture M4) shows an increase of 7.5% in mechanical strength comparing to the R pastes with 28 days age, this is because of the SF is a non-crystalline material with a high surface area, which make it an excellent puzzolanic material and also during the initial reactions can act as nucleation sites by increasing the reaction rate and precipitation of gel CSH, this promoting the increase in compressive strength. This behavior has been reported in other studies with the use of SF in concrete [45,46]

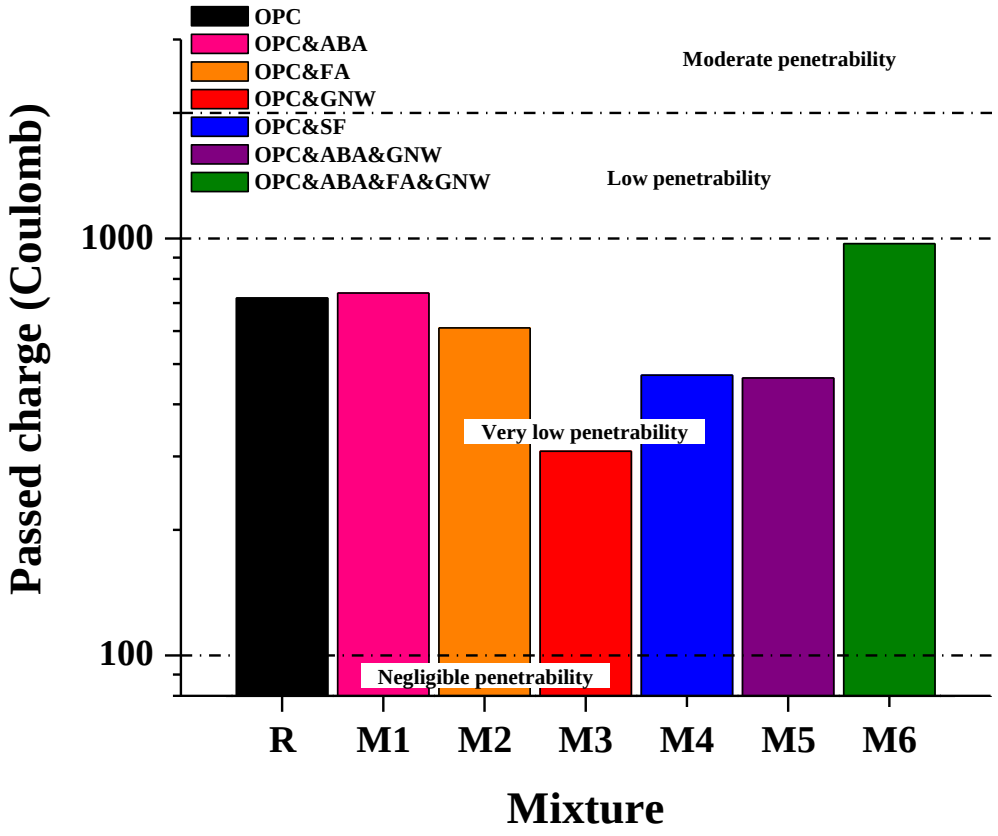

Figure 2. Resistance to chloride ion penetration of pastes at 28 days of age.

On the other hand, the pastes additioned with ABA shows an increase in compressive strength with respect to time and the same as the rest of pastes, also they showed higher values than R pastes, as in the case of pastes additioned with 5% ABA (mixture M1), which exceeded in compressive strength of 13.95% over the R pastes. This is because the limestone filler support during the process of accelerating cement hydration manifests as Lothenbach et al [47] and later on De Weerdt et al [48]. In addition, Li et al [49] observed a substantial increase in the mechanical strength of concrete when auditioned 3% of nano-limestone getting 140 MPa of mechanical strength compared against 125.6 MPa in reference concretes, represents an increase in compressive strength of ~12%. Also,

Ramezanianpour et al [50], they observed that at the age of 28 days, the mechanical strength of concretes additioned with 5% of limestone overcame the concretes elaborated with 100% OPC and this behavior repeated at age of 90 and 180 cured days.

In the figure 2, the results of passed charge according to the ASRM C1202 procedure of test are presented. Generally, in figure 2 can be seen that the mixtures showed a very low penetrability resistance of Cl^- ion according with ASTM C1202 parameters, since all are in range charger of 100-1000 Coulombs. Nevertheless the mixtures showed differences on their charger values, such is the case of pastes additioned with 5% of GNW (Mixture 3) that showed a charge on the range of 309 Coulombs, they have the highest penetrability resistance of Cl^- ion exhibited, load the values charge represented a penetration of 8.52 mm according with post-mortem studies in the pastes (see figure 3). This indicates that the use of GNW in pastes provides a great capacity to inhibit the chloride ions penetration, because the charge passed in the mixture is 57.08% smaller than the mixture R (100% OPC, 720 Coulombs, 14.32 mm of chloride ion penetrability).

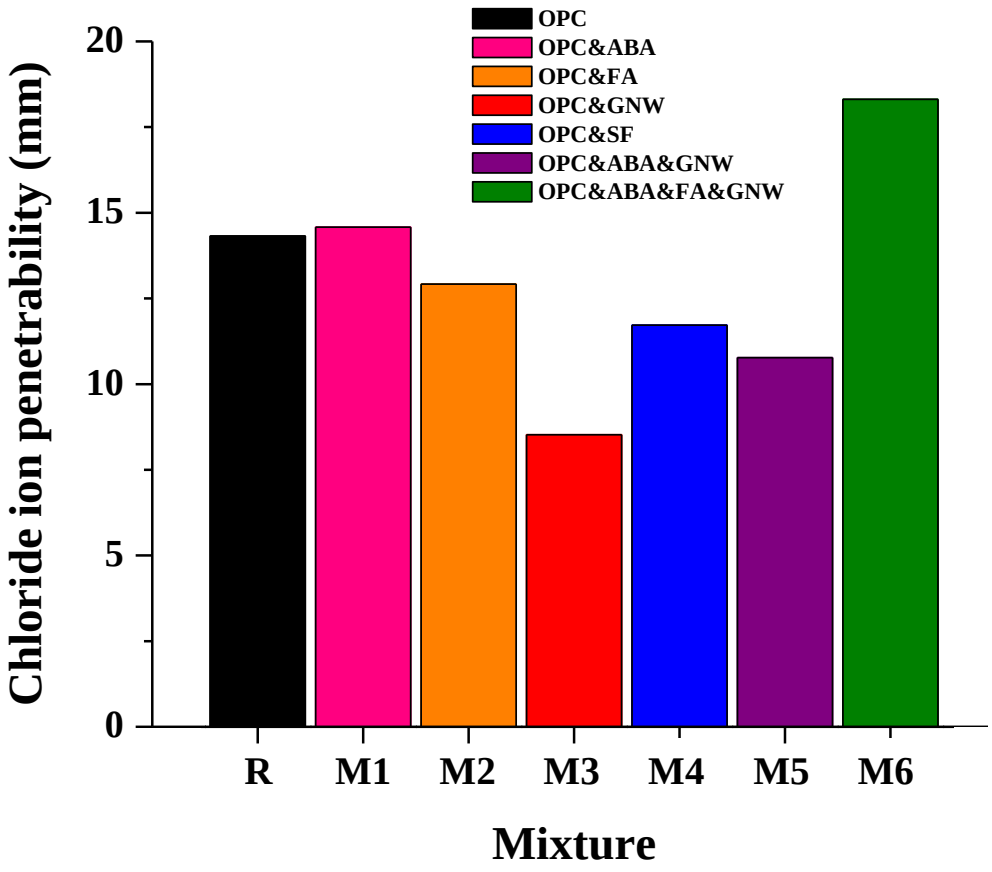

Figure 3. Penetration of Chloride ion in the pastes after RCPT.

Similar behavior was observed in mixtures M2 (5% FA, 610 Coulombs, 12.92 mm of chloride ion penetrability), M4 (5% SF, 470 Coulombs, 11.72 mm of chloride ion penetrability) and M5 (2.5% ABA and 2.5% GNW, 463 Coulombs, 10.77 mm of chloride ion penetrability) since they had smaller charge than mixture R (100% OPC) on a 15.27%, 34.72% and 35.69% respectively. Similar behavior has been observed in other investigations in which has been used nanosilica as supplementary material

in the production of mortars, which exhibit a greatly decreased on the chloride penetration respect to the reference mortars [51,52]. Also, the penetrability of concrete usually decreases with the addition of the supplementary cementitious materials such as fly ash or silica fume [53,54].

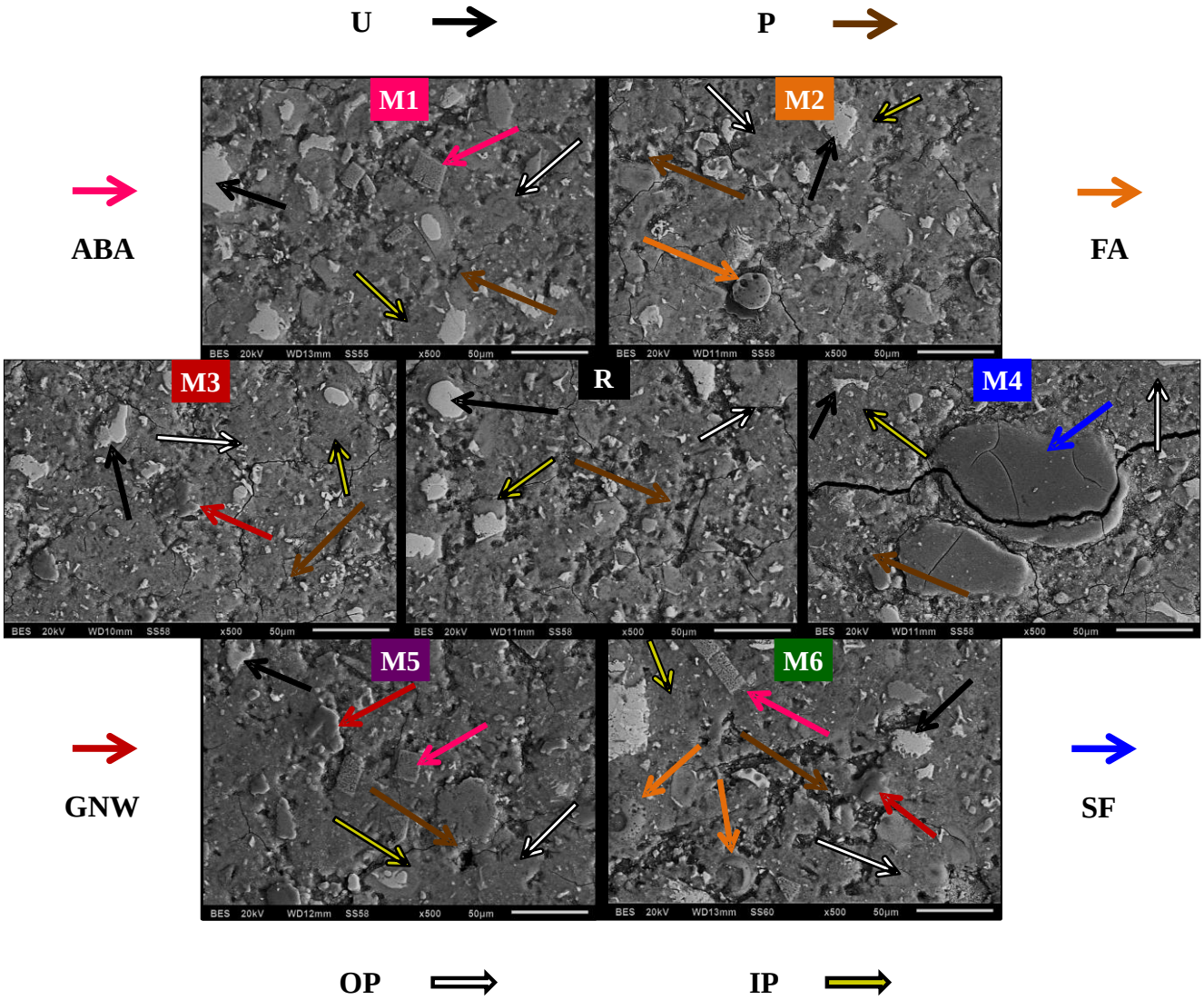

Figure 4. Microstructural comparison of all pastes curing at 28 days: ABA (pink arrow), FA (orange arrow), GNW (red arrow) and SF (blue arrow); inner product CSH (IP, black and yellow arrow), outer product CSH (OP, white and black arrow), unreacted cement (U, black arrow) and porosity (P, brown arrow).

Furthermore, the mixture M1 (5% ABA, 740 Coulombs, 14.58 mm of chloride ion penetrability) and M6 (1.67%ABA&1.67%FA&1.67%GNW), 971 Coulombs, 18.31 mm of chloride ion penetrability) showed a small increase in the load values regarding the mixtures references, this increase represents 2.7% and 25.84% respectively. Some authors have reported that the penetration of chloride ion increases in concretes containing 10%, 15% and 20% of limestone [55,56].

The figure 4 show a comparative regarding the microstructure exhibited for each pastes at age of 28 days and it was obtained by scanning electron microscopy (SEM) using back-scattered electron

(BSE) detector and magnification of 500X. In figure 4 the OPC replaced materials are identified of the next way: ABA (pink arrow), FA (orange arrow), and SF (blue arrow); also, the CSH gel on the modality of inner product (IP, black and yellow arrow) and outer product (OP, white and black arrow), unreacted cement (U, black arrow) and porosity (P, brown arrow).

In general, it can be seen that the R pastes (100% OPC) present a lot of cement grain in hydration process (U), as well lots of pores (P), this in comparison to the rest of the pastes. Similar behavior is seen in mixtures M1 (5% ABA) and M6 (1.67 ABA & 1.67 FA & 1.67 GNW), although the latter was added with pozzolanic materials such as FA and GNW. These R pastes, M1 and M6 exhibited the highest values in porosity, 16.98%, 17.17% y 17.65%, respectively (seen figure 5), values that agree with the obtained results from resistance to chloride ion penetration (passed charge) and the post-mortem study of the pastes under the chemical interaction with silver nitrate ($AgNO_3$) as indicator of chloride ion penetration (penetrability).

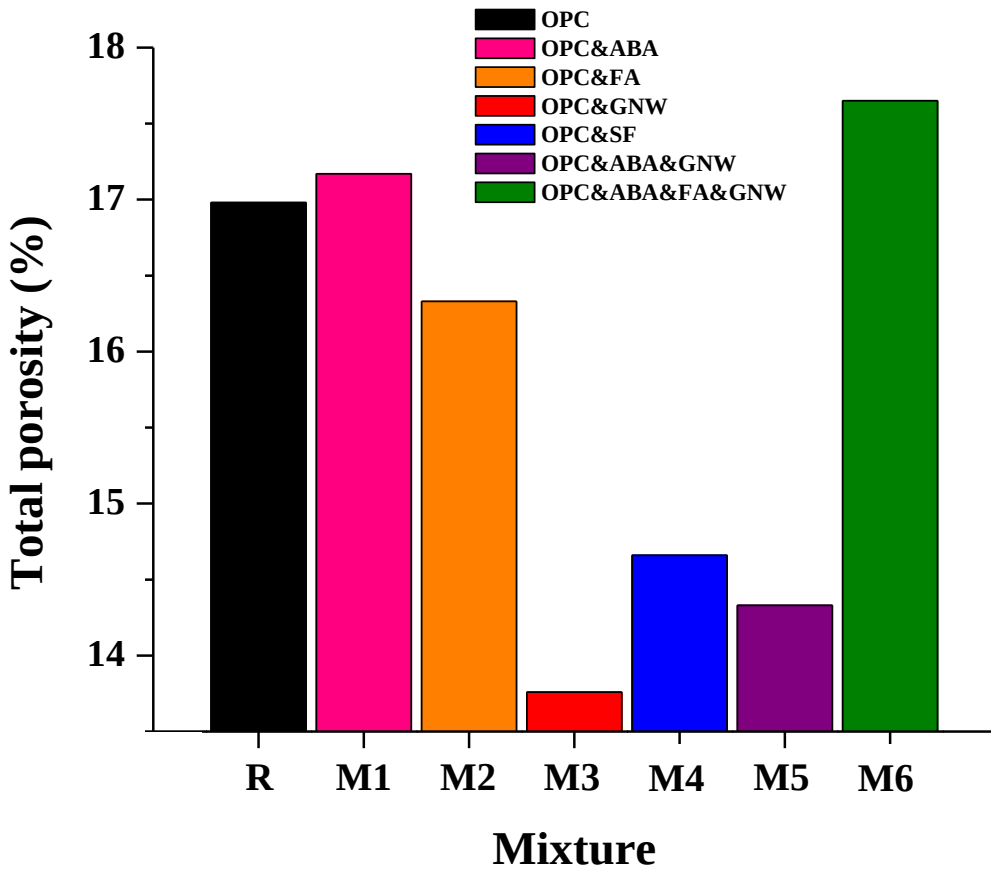

Figure 5. Total porosity of pastes at 28 days of age.

This slight increase in porosity obtained in pastes M1 for R pastes can be attributed to ABA particles because they have rectangular fibrous morphology in order of 20 and 40 μm which present internal porosity, as pores in their around (interface between ABA and hydrates) as can be observed in the images of figure 4 where pink arrow show ABA particles. This phenomenon has been previously reported in other investigation in pastes added with limestone and they have been analyzed

microstructurally at ages of 7 and 28 days [57,58]. Similar behavior suggests it was lead on pastes M6 because the material addition is the ABA, nevertheless the puzzolanic reaction effects from other materials in addition (FA and GNW) with calcium hydroxide was not expected as these contributed to the low formation CSH gel to densify the cementitious matrix, so that the decrease of the porosity was not favored as expected.

Additionally, the pastes added with GNW at 2.5% to 5% wt, present a more compact microstructure, due to the strong pozzolanic reaction between GNW and calcium hydroxide that made additional CSH gel, contributing to decrease the porosity, as reflected by the results in pastes M3 and M5, which present a low porosity values, 13.76% and 14.33% respectively (figure 5). This effect of microstructure densification of the pastes using nano-silica has been reported by others authors [59,60]. Finally the pastes additioned with SF to 5% (M4) show a less compact microstructure as we expected, so that the porosity developed (14.66%) was higher than the pastes presented with added GNW. In addition, the microstructure show lot of agglomerates of SF particles that exceed 50 μm, promoting the reaction of silica phenomenon that contributed to the results of properties mechanical, which show poor gain strength over the reference pastes (R) associated with low reactivity for the additional generation of CSH gel. The RAS phenomenon has been widely reported by other authors, which contribute very negatively on the overall properties of concretes [61,62].

3. CONCLUSIONS

These results revealed that geothermal nano-SiO_2 waste (GNW) and limestone of agave bagasse ash (ABA) could be a potentially suitable material for making pastes, mortars and concrete with industrial applications, which will contribute positively to the reduction of the CO_2 emissions into the atmosphere, as well as decrease the environmental impact generated at the disposal zones. Because together they showed enhanced mechanical properties and lower porosity, permeability chloride and high resistance to passed charge, compared with pastes made with OPC 100% and additoned with silica fume (SF) and fly ash (FA).

Mechanical property results showed that it is possible to use GNW up 5% as a replacement of OPC, because it provides a high enhancement of compressive strength that exceed of pastes elaborated with 100% OPC in ~45%, as well as the pastes additioned with SF at 5% in ~40% more. Also, that it is possible to use of ABA up 5% because exceed in ~15% of compressive strength than pastes of 100% OPC. Likewise, the ternary (OPC&ABA&GNW) and quaternary (OPC&ABA&FA&GNW) systems exhibited 35% and 20% additional of compressive strength of pastes of 100% OPC respectively.

The RCPT results indicate that pastes additioned with GNW have a less open structure of pores than reference pastes. In this sense, the use of GNW in 5% (OPC&GNW) and 2.5% (OPC&ABA&GNW) outcomes in a decrement in the passed charge through the pastes in 57% and 35%, respectively, this compared whit paste reference. Similar behavior was exhibited by pastes mixed with SF and FA whose values in charge, 35% and 15% respectively, were lower than pastes of OPC 100%. However, this behavior was not observed in pastes mixed with ABA because these increased

slightly the passed charge in 3% (OPC&ABA) and 25% (OPC&ABA&FA&GNW) more than pastes of OPC 100%.

The microstructural analysis showed that pastes elaborated with GNW exhibited a higher densification of CSH gel, due to the strong pozzolanic reaction of GNW to calcium hydroxide generating CSH gel additional obtaining with this a matrix with less porosity compared with the 100% OPC. These effects occurred in pastes mixed with SF and FA but the pozzolanic reaction was poor in comparison with that generated by GNW, thus reflecting small increases in porosity values respect to porosity of GNW but less compared with the 100% OPC. However, this behavior was not observed in pastes additioned with ABA due to the porosity developed around the particles of ABA, exhibiting less compact and more porous scantily microstructures than those presented in pastes of OPC 100%.

References

1. E. M. R. Fairbairn, B. B. Americano, G. C. Cordeiro, T. P. Paula, R. D. Toledo Filho, M. M. Silvoso, *J. Environ. Manage*, 91 (2010) 1864-1871.
2. C. A. Hendriks, E. Worrell, D. De Jager, K. Blok, P. Riemer, *Greenhouse gas control technologies conference paper-cement*, August (2004).
3. M. Nehdi, J. Duquette, A. El Damatty, *Cem. Concr. Res.*, 33 (2003) 1203-1210.
4. D. Anderson, A. Roy, R. K. Seals, F. K. Cartledge, H. Akhter, S. C. Jone, *Cem. Concr. Res.*, 30 (2000) 437-445.
5. V. M. Malhotra, *Proceedings of a Symposium Honoring Prof Raymundo Riverá-Villarreal International Symposium on Durability of Concrete*, Monterrey México, May (2005).
6. A. Cwirzen, V. Penttala, C. Vornanen, *Cem. Concr. Res.*, 38 (2008) 1217-1226.
7. K. Sisomphon, L. Franke, *Cem. Concr. Res.*, 37 (2007) 1647-1653.
8. R. Corral-Higuera, S. P. Arredondo-Rea, M. A. Neri-Flores, J. M. Gómez-Soberón, J. L. Almaral-Sánchez, J. H. Castorena-González, A. Martínez-Villafañe, F. Almeraya-Calderón, *Int. J. Electrochem. Sci.*, 6 (2011) 958-970.
9. E. I. Moreno, R. G. Solís-Carcaño, J. Varela-Rivera, J. C. Pacho-Monforte, R. A. Cua-Cuevas, *Int. J. Electrochem. Sci.*, 10 (2015) 6444-6453.
10. M. J. Pellegrini-Cervantes, C. P. Barrios-Durstewitz, R. E. Nuñez-Jaquez, S. P. Arredondo-Rea, F. J. Baldenebro-Lopez, M. Rodríguez- Rodríguez, L. G. Ceballos-Mendivil, A. Castro-Beltrán, G. Fajardo-San-Miguel, F. Almeraya-Calderon, A. Martinez-Villafañe, *Int. J. Electrochem. Sci.*, 10 (2015) 332-346.
11. O. D. Whitescarver, J. T. Kwan, K. M. Chan, D. P. Hoyer, *Patent: "Process for using sludge from geothermal brine to make concrete and concrete composition"*, United States Patent 4900360, California (1990).
12. A. Camenzuli, G. M. Mudd, *3rd International Conference on Sustainability Engineering & Science: Blueprints for Sustainable Infrastructure Auckland*, New Zealand, December (2008).
13. Comisión Federal de Electricidad, http://www.cfe.gob.mx.
14. L. Y. Gómez, J. I. Escalante, G. Mendoza, *Journal of Materials Science Letters*, 39 (2004) 4021-4025.
15. J. Rincon, M. Romero, C. Díaz, V. Balek, Z. Malek, *J. Therm. Anal. Calorim.*, 56 (1999) 1261-1269.
16. L. Y. Gómez, J. I. Escalante, *12th International Congress on the Chemistry of Cement*, Canada (2007).

17. R. Puente-Ornelas, L. Y. Gómez-Zamorano, M. C. Alonso, P. C. Zambrano, A. M. Guzmán, E. Rodríguez, B. Bermúdez-Reyes, M. Sánchez-Moreno, *Int. J. Electrochem. Sci.*, 7 (2012) 136-149.
18. C. A. Iñiguez-Sanchez, L. Y. Gómez-Zamorano, M. C. Alonso, *J. Mater. Sci.*, 47 (2012) 3639-3647.
19. C. G. Iñiguez, C. J. J. Bernal, M. W. Ramirez, N. J. Villalvazo, *Advances in Chemical Engineering and Science*, 4 (2014) 135-142.
20. E. B. Ibarra-Hernández, J. F. Botero González, C. Cortez Amador, *Ingeniería de tequilas 1ª Edición*, Bogotá, Colombia (2010) 12-37.
21. L. Chávez, *Ingenierías*, 8 (2010) 8-16.
22. B. E. Barragán-Huerta, Y. A. Téllez Díaz, A. Laguna Trinidad, *Revista Sistemas Ambientales*, 2 (2008) 44-50.
23. A. M. Sánchez-Riano, A. I. Gutiérrez -Morales, J. A. Muñoz-Hernández, C. A. Rivera-Barrero, *Tombaga*, 5 (2010) 61-91.
24. L. Chávez-Guerrero, M. Hinojosa, *Fuel*, 89 (2010) 4049–4052.
25. L. Chávez-Guerrero, J. Flores, B. I. Kharissov, *Chemosphere*, 81 (2010) 633–638
26. A. Heredia-Solís, E. Esparza-Ibarra, L. Romero-Bautista, F. Cabral-Arellano, R. Bañuelos-Valenzuela, *ReIbCi*, 1 (2014) 103-110.
27. C. Huitron, R. Perez, A. E. Sanchez, P. Lappe, L. Rocha Zavaleta, *Journal of Environmental Biology*, 29 (2008) 37-41.
28. R. Puente Ornelas, L. Chávez Guerrero, P. Zambrano Robledo, M. Lara Banda, *12th Interamerican Microscopy Congress CIASEM 2013*, Cartagena de Indias, Colombia, Septiembre (2013).
29. J. R. González-López, J. F. Ramos-Lara, A. Zaldivar-Caden, L. Chávez-Guerrero, R. X. Magallanes-Rivera, O. Burciaga-Díaz, *Fuel Processing Technology*, 133 (2015) 35-42.
30. ASTM C618-08a: *"Standard Specification for Coal Fly Ash and Raw or Calcined Natural Pozzolan for Use in Concrete", ASTM International* (2008).
31. D. Skoog, D. West, F. Holler, *Química Analítica*, 6 Ed. Mc Graw-Hill, México (1995).
32. NMX C-414-ONNCCE: *"Industria de la construcción, cementos hidráulicos, especificaciones y métodos de prueba", Organismo Nacional de Normalización y Certificación de la Construcción y Edificación, S.C.* (2003).
33. ASTM C-642-97: *"Standard Test Method for Density, Absorption, and Voids in Hardened Concrete", ASTM International* (1997).
34. ASTM C1202-10: *"Standard Test Method for Electrical Indication of Concrete's Ability to Resist Chloride Ion Penetration", ASTM International* (2010).
35. L. Senff, J. A. Labrincha, V. M. Ferreira, D. Hotza, W. L. Repette, *Construction and Building Materials*, 23 (2009) 2487-2491.
36. J. Shih, T. Chang, T. Hsiao, *Materials Science and Engineering A*, 424 (2006) 266-274.
37. G. Quercia, H. J. H. Brouwers, *8th fib International PhD Symposium in Civil Engineering*, Technical University of Denmark, Kgs. Lyngby, 20-23 June (2010) 1-6.
38. Y. Qing, Z. Zenan, K. Deyu, Ch. Rongshen, *Construction and Building Materials*, 21 (2007) 539–545.
39. K. L. Lin, W. C. Chang, D. F. Lin, H. L. Luo, M. C. Tsai, *Journal of Environmental Management*, 88 (2008) 708–714.
40. M. Ahmaruzzaman, *Progress in Energy and Combustion Science*, 36 (2010) 327-363.
41. P. Chindaprasirt, C. Jaturapitakkul, T. Sinsiri, *Cem. Concr. Compos.*, 27 (2005) 425-428.
42. M. K. Golapan, *ACI Materials Journal*, 90 (1993) 117-21.
43. G. C. Isaia, A. L. G Gastaldini, R. Morales, *Cem. Concr. Compos.*, 25 (2003) 69-76.
44. S. Slanicka, *Cem. Concr. Res.*, 21 (1999) 285-296.
45. A. A. Almusallam, H. Beshr, M. Maslehuddin, O. S. B. Al-Amoudi, *Cem. Concr. Compos.*, 26 (2004) 891–900.
46. J. Zelić, D. Rušić, D. Veza, R. Krstulović, *Cem. Concr. Res.*, 30 (2000) 1655-1662.

47. B. Lothenbach, G. Le Saout, E. Gallucci, K. Scrivener, *Cem. Concr. Res.*, 38 (2008) 848–860.
48. K. De Weerdt, M. Ben Haha, G. Le Saout, K.O. Kjellsen, H. Justnes, B. Lothenbach, *Cem. Concr. Res.*, 41 (2011) 279–291.
49. W. Li, Z. Huang, F. Cao, Z. Sun, S. P. Shah, *Construction and Building Materials*, 95 (2015) 366–374.
50. A. A. Ramezanianpour, E. Ghiasvand, I. Nickseresht, M. Mahdikhani, F. Moodi, *Cem. Concr. Compos.*, 31 (2009) 715–720
51. D. Kong, X. Du, S. Wei, H. Zhang, Y. Yang, S. P. Shah, *Construction and Building Materials*, 37 (2012) 707–715.
52. X. He, X. Shi, *J Transp Res Board*, 2070 (2008)13–21.
53. S. Mindess, J. F. Young, D. Darwin, *Concrete*, second ed. Prentice Hall, New Jersey, USA (2002).
54. P. V. Den Heede, M. Maes, N. De Belie, *Construction and Building Materials*, 67 (2014) 74–80
55. M. Ghrici, S. Kenai, M. S. Mansour, *Cem. Concr. Compos.*, 29 (2007) 542–549.
56. V. Bonavetti, H. Donza, V. Rahhal, E. Irassar, *Cem. Concr. Res.*, 30 (2000) 703-708.
57. G. Ye, X. Liu, G. De Schutter, A. M. Poppe, L. Taerwe, *Cem. Concr. Compos.*, 29 (2007) 94–102.
58. G. Menéndez, V. Bonavetti, E. F. Irassar, *Cem. Concr. Compos.*, 25 (2003) 61–67.
59. M. Zahedi, A. A. Ramezanianpour, A. M. Ramezanianpour, *Construction and Building Materials*, 78 (2015) 354–361
60. H. Du, S. Du, X. Liu, *Construction and Building Materials*, 73 (2014) 705–712
61. A. J. Maas, J. H. Ideker, M. C. G. Juenger, *Cem. Concr. Res.*, 37 (2007) 166-174.
62. L. Y. Gomez-Zamorano, J. I. Escalante, *Materiales de Construcción*, 59 (2009) 5-16.